ORNL/TM-2020/1765
CRADA/NFE-18-07409

Catalytic Pulping of Wood

Jerry M. Parks

September 29, 2020

OAK RIDGE NATIONAL LABORATORY
MANAGED BY UT-BATTELLE FOR THE US DEPARTMENT OF ENERGY

DOCUMENT AVAILABILITY

Reports produced after January 1, 1996, are generally available free via US Department of Energy (DOE) SciTech Connect.

Website http://www.osti.gov/scitech/

Reports produced before January 1, 1996, may be purchased by members of the public from the following source:

National Technical Information Service
5285 Port Royal Road
Springfield, VA 22161
Telephone 703-605-6000 (1-800-553-6847)
TDD 703-487-4639
Fax 703-605-6900
E-mail info@ntis.gov
Website http://www.ntis.gov/help/ordermethods.aspx

Reports are available to DOE employees, DOE contractors, Energy Technology Data Exchange representatives, and International Nuclear Information System representatives from the following source:

Office of Scientific and Technical Information
PO Box 62
Oak Ridge, TN 37831
Telephone 865-576-8401
Fax 865-576-5728
E-mail reports@osti.gov
Website http://www.osti.gov/contact.html

This report was prepared as an account of work sponsored by an agency of the United States Government. Neither the United States Government nor any agency thereof, nor any of their employees, makes any warranty, express or implied, or assumes any legal liability or responsibility for the accuracy, completeness, or usefulness of any information, apparatus, product, or process disclosed, or represents that its use would not infringe privately owned rights. Reference herein to any specific commercial product, process, or service by trade name, trademark, manufacturer, or otherwise, does not necessarily constitute or imply its endorsement, recommendation, or favoring by the United States Government or any agency thereof. The views and opinions of authors expressed herein do not necessarily state or reflect those of the United States Government or any agency thereof.

ORNL/TM-2020/1765
CRADA/NFE-18-07409

Biosciences Division

Molecular Modeling to Increase Kraft Pulp Yield

Brandon Knott (NREL)
Jerry M. Parks (ORNL)
Adriaan van Heiningen (U Maine)
and
David B. Turpin (APPTI)

Date Published:
September 29, 2020

Prepared by
OAK RIDGE NATIONAL LABORATORY
Oak Ridge, Tennessee 37831-6283
managed by
UT-BATTELLE, LLC
for the
US DEPARTMENT OF ENERGY
under contract DE-AC05-00OR22725

Approved for public release

Abstract
Kraft pulping is an important component of the pulp and paper industry and is the predominant technology for removing lignin from wood carbohydrates. However, kraft pulping is energy-intensive, expensive, and is limited by the degradation of cellulose and hemicellulose. Pretreatment increases yield by stabilizing cellulose against degradation. However, protection of galactoglucomannan (GGM), the primary hemicellulose component of softwood, is minimal when conventional pretreatments are used. Here we investigate the effectiveness of new pretreatment methods on southern pine wood chips under a range of experimental conditions. If successful, improved pretreatment methods will increase carbohydrate yield, reduce waste, reduce energy use, lower the cost of bleaching, and decrease the cost of air emission controls. The purpose of this CRADA was to combine industrial expertise in wood pulping with national laboratory expertise in high-performance computing, leading to improved understanding of molecular-scale processes that limit carbohydrate yield during pretreatment and pulping. A combined computational and experimental approach was used to investigate pretreatment effectiveness under relevant pulping conditions and then use molecular simulation techniques to provide complementary insight into structural and chemical factors that govern the observed behavior. In this report we summarize the accomplishments of the project.

Statement of Objectives
The Alliance for Pulp and Paper Technology Innovation (APPTI) is an industry-led consortium that promotes the development of advanced manufacturing technologies for the pulp and paper industry. Among the main objectives of APPTI are to identify high-priority technology challenges for the pulp and paper industry and to promote pre-competitive scientific R&D projects to address those challenges. The goals of the organization are to reduce water consumption and enhance water reuse, reduce energy use and carbon emissions, increase manufacturing process efficiency, improve raw material yield, and develop new bio-based products.

The pulp and paper industry is essential for making products necessary for everyday life from renewable resources. Kraft pulping, the predominant technology for removing lignin from wood carbohydrates, is based on dissolution of lignin from wood by reaction at high temperature (150-170°C) with an aqueous solution of NaOH and Na_2S. Unfortunately, this process is energy-intensive, capital-intensive, and provides a less efficient use of wood resources than desired due to substantial degradation of hemicelluloses and cellulose.

The purpose of chemical pulping is to remove lignin from cellulosic biomass while preserving polysaccharides required for pulp strength. Lignin is a naturally occurring polymer in wood that must be removed to expose the polysaccharides used in the pulping industry to produce paper products. Kraft pulping, the predominant technology, is capital- and energy-intensive, and it provides a less efficient use of wood resources than desired.

Wood is composed of 40-45% cellulose, 25-30% hemicellulose, and 25-30% lignin, whereas the final kraft pulp consists of 35-40% cellulose, 8-13% hemicellulose, and 1-2% lignin. Cellulose is a homopolymer consisting of repeating D-anhydroglucopyranose units linked by β-1,4 glycosidic bonds (**Figure 1**). In contrast, galactoglucomannan (GGM), the primary hemicellulose in softwood, is a heteropolymer consisting of uneven β-1,4-linked glucose and mannose as a backbone with some mannose units substituted by α-1,6-linked galactose.

Wood remains the largest cost in the manufacture of wood pulp for paper, and increasing pulp yield has the largest financial impact on pulp mill economics. Increasing kraft pulp yield would improve energy efficiency, increase mill profitability, and preserve jobs (this industry employs 378,000 American workers). For example, increasing pulp yield to 50% from the current 45% would decrease the energy intensity by ~10% (13T BTU/year), corresponding to ~$33M, and also reduce carbon emissions.

A 5% yield increase has never been achieved because the alkaline lability of wood carbohydrates promotes peeling reactions wherein sugars are lost ("peeled") from carbohydrate chain ends. Softwood pretreatment with methyl mercaptide (MM) has been demonstrated to increase yield by 3% primarily by stabilizing cellulose against degradation by alkaline peeling (general reaction scheme shown in **Figure 1**). Unfortunately, galactoglucomannan (GGM, the primary hemicellulose molecule in softwood) stabilization by this pretreatment is minimal, and thus represents a promising target for increasing the overall preservation of wood carbohydrates and thus increasing yield.

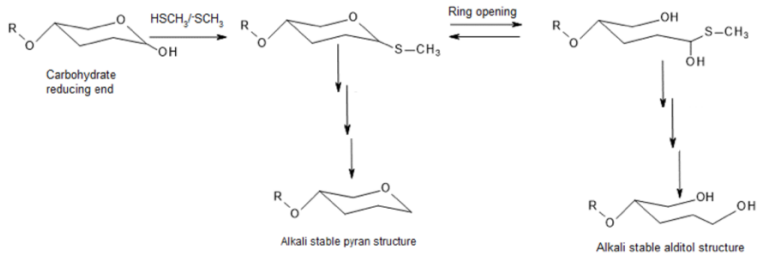

Figure 1. Reducing end group (REG) stabilization by methyl mercaptan.

In the current work, a fundamental understanding of the MM and alkali reactivity of wood components has been elucidated via a multi-pronged molecular modeling approach involving molecular dynamics simulations and density functional theory reaction mechanism calculations. We report reaction pathways and kinetics of pretreatment reactions for model structures representing the biomass polysaccharides GGM and cellulose. Evaluation of the reactivity of these species reveals sites of reaction, thermodynamics, and kinetics, demonstrating how and why the pretreatment chemistry selectively interrupts the peeling reaction for cellulose and how the analogous reactions of native GGM might be controlled. Kinetic data and quantitative product analysis of pretreated real wood chips provided by the University of Maine (PI Adriaan van Heiningen) enable validation and comparison of computational setup and results.

Here, we leveraged ORNL high-performance computing expertise and resources to investigate the mechanisms of cobalt-salen catalysts for mild and efficient oxidative delignification of lignin model compounds.

In this project, the Participant (APPTI) and Contractors (NREL, ORNL and U. Maine) sought to integrate HPC with conventional experimental approaches to evaluate and optimize pretreatment approaches that provide increased yields of carbohydrates from paper pulping relative to existing pretreatment strategies.

The Contractors and Participant participated in regular conference calls.

Benefits to the Funding DOE Office's Mission

The mission of the DOE Office of Science is to deliver the scientific discoveries and major scientific tools that transform our understanding of nature and advance the energy, economic, and national security of the United States. The work performed in this CRADA specifically benefits the DOE mission in renewable energy, high-performance computing, and energy efficiency in manufacturing.

Technical Discussion of Work Performed by All Parties

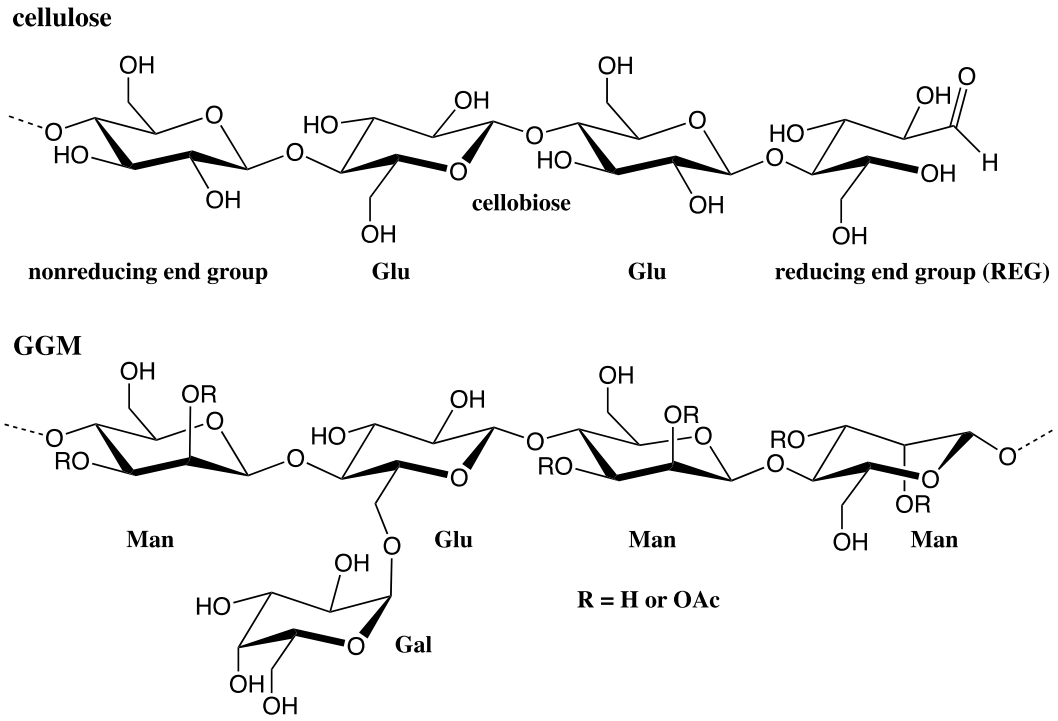

Figure 1. Chemical structures of cellulose and galactoglucomannan (GGM).

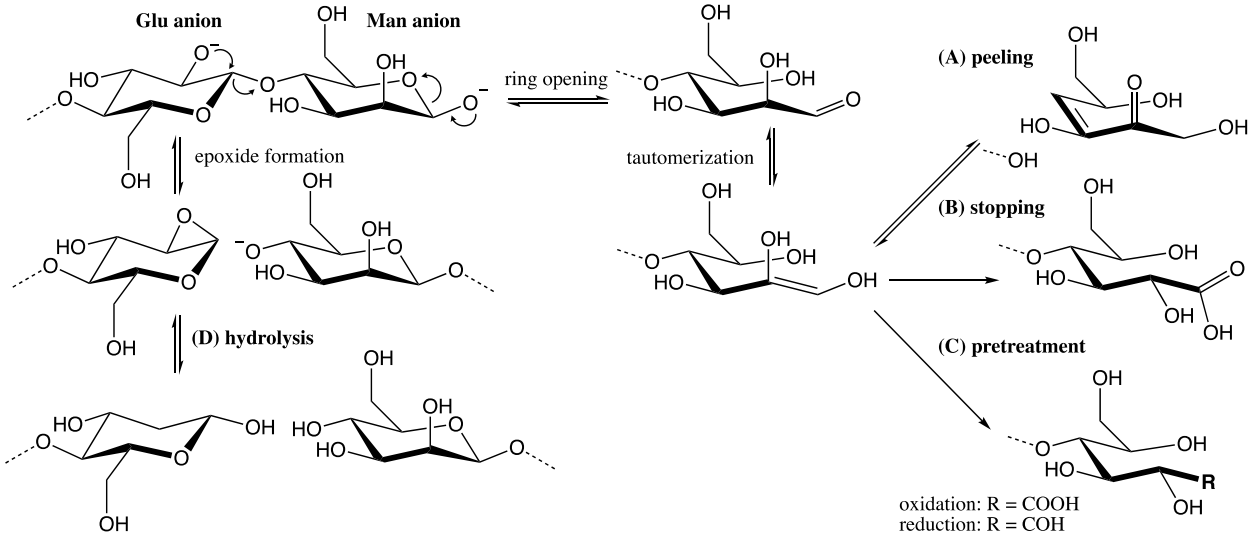

Figure 2. Selected reactions for (**A**) peeling, (**B**) stopping, (**C**) pretreatment, and (**D**) hydrolysis.

At high pH, the reducing end groups (REGs) of cellulose and hemicellulose (glucomannan and xylan) polymers undergo a stepwise depolymerization reaction called primary peeling, leading to undesired loss of carbohydrates (**Figure 2**). Primary peeling of cellulose becomes significant above 130°C (Paananen, 2010; Nieminen, 2014). However, primary peeling of GGM begins around 80°C (Montagna, 2013). Chain ends can also undergo stopping reactions, in which the reducing end groups are converted into alkali-stable carboxylate groups. In addition, internal glycosidic bonds in a polysaccharide chain are susceptible to chain

breakage by alkaline hydrolysis. When hydrolysis occurs, one of the newly formed chain ends is a reducing end group that can then undergo further stepwise degradation, i.e., secondary peeling.

Various approaches have been developed to minimize primary peeling of carbohydrates by converting the reducing end groups into alkali-stable groups through both oxidative and reductive reactions. Oxidative pretreatments include the use of anthraquinone or polysulfides (Wang, 2015). Criteria for a suitable pretreatment include (i) low cost (or efficient recoverability), (ii) no non-process elements (i.e., only H, C, O, S and Na, and (iii) it should be a reductant, which does not result in the formation of unsaturated bonds that can undergo further peeling (Linden, 2020). A common reductive pretreatment involves the use of sodium borohydride, which is expensive and adds the non-process element boron to the reaction conditions (Wang, 2015). Recently, sodium dithionite was investigated but was unsuccessful in stabilizing mannose under kraft pulping conditions (Linden, 2020).

Temperature, alkali, and other pulping conditions all influence the amounts of peeling, stopping, and hydrolysis. Numerous kinetic models have been developed to predict carbohydrate degradation during pulping (Paananen, 2010; Nieminen, 2014; Fearon, 2020; Silva-Perez, 2015). Although these models provide valuable information, molecular-scale simulation is a complementary technique that can provide detailed molecular insight. Molecular dynamics simulation studies have investigated various aspects of carbohydrate conformations and dynamics in aqueous solution at the molecular scale (Kraütler, 2007; Peric-Hassler, 2010; Berglund, 2016;
Berglund, 2019).

Here we use aqueous sodium methylmercaptide as a pretreatment for wood chips under various conditions relevant to pretreatment and pulping. We perform a quantitative product composition analysis and show that sodium methylmercaptide is an effective pretreatment for improving carbohydrate yield, but that it is substantially less effective for GGM than for xylose and cellulose. To investigate various aspects of carbohydrate conformations and dynamics under process-relevant conditions, we perform molecular dynamics simulations of cellulose and GGM. We then perform quantum mechanical calculations to investigate mechanistic details of the peeling reaction and alkaline hydrolysis.

Experimental Methods

Pulping experiments were performed using southern pine chips obtained from US mills. All experiments were performed in quadruplet using four 235 mL cylindrical rocking digesters. About 30 grams of wood chips (on oven dry basis) was used in each digester. To avoid the handling of methyl mercaptan (MM) gas, an aqueous solution of sodium methyl mercaptide (SMM, 21% w/w) containing a small amount of NaOH (0.4% w/w) at pH 12.9 was obtained from Arkema (King of Prussia, PA 19406). The SMM charge (calculated as MM) was 1 to 6% on wood (oven dry) basis. The liquor-to-wood ratio for MM pre-treatment was 3 L/kg and the pre-treatment temperature was between 80°C to 130°C, depending upon the experiment.

At the end of pre-treatment, the digesters were cooled to room temperature (using a water bath) while make-up white liquor was being prepared. The final pH of the pre-treatment liquor was between 9.5 to 10.5. The total liquor-to-wood ratio after adding make-up white liquor was 4.5 L/kg. It should be noted that for some experiments the SMM solution was charged together with the make-up white liquor to simulate more practical pulp mill conditions. After adding the make-up white liquor (sulfidity: 30%, causticization efficiency: 80%), the digesters were placed in the oil bath for 1 hr at 115°C to achieve impregnation of white liquor into chips. At the end of impregnation, the digesters were removed from the oil bath and cooled to room temperature while the oil bath was being heated to the cooking temperature of 170°C. The digesters were then immersed in the bath and cooked to a target H-factor of ~1960 hr.

Screened pulp was used to determine the kappa number (TAPPI Standard T-236) and chemical composition. The carbohydrate composition of wood and pulp was determined using high-performance anion exchange chromatography (HPAEC) after acid hydrolysis of the pulp sample. TAPPI standard methods (T-249, T-222, and T-204) were used to estimate the composition of lignin and extractives in the wood/pulp samples. The uronic anhydride content was determined using the chromophoric group analysis method (Scott, 1979). Residual alkali was determined using a modified SCAN-N 2:88 method.

Computational Methods

Molecular dynamics (MD) model construction. To construct the complex model of GGM bound to cellulose, a 36-chain cellulose I_β microfibril model with degree of polymerization (DP) of 20 was first generated with a diamond cross-sectional geometry (**Figure 3**). Subsequently, 18 GGM molecules with DP of 15 were then pseudo-randomly arranged around the cellulose microfibril, resulting in a cellulose/GGM ratio of 2.7, which is consistent with the experimentally observed cellulose/GGM ratio of ~2.6 (Negahdar, 2016). Our model constructs a GGM molecule as being composed of three repeat units, each consisting of three mannose residues, one glucose residue, and one galactose residue. The galactose residue is attached to the glucose residue at the backbone by an α-1,6-linkage. In addition, because cellulose is a simple homopolymer consisting of repeating D-anhydroglucopyranose units linked by β-(1,4)-glycosidic bonds, we used a β-(1,4)-glycosidic bonded glucose dimer (Glu-Glu) to represent the cellulose for additional MD simulations and subsequent quantum mechanical calculations (**Figure 3C**). GGM is a heteropolymer consisting of uneven β-(1,4)-linked glucose and mannose as a backbone with some mannose units substituted by α-(1,6)-linked galactose. The molar ratio 'galactose:glucose:mannose' in GGM is approximately 1:1:3. Because of the 1:3 molar ratio between glucose and mannose, we used β-(1,4)-linked mannose dimer (Man-Man) instead of glucose-mannose dimer to represent GGM (**Figure 3C**). However, β-(1,4)-linked Glu-Man was used in some cases as a model of GGM for the quantum mechanical calculations of alkaline hydrolysis (see below). The dimer simulations were constructed, along with pretreated forms of Glu-Glu and Man-Man dimers (**Figure 3D**), both for computational efficiency and also to remove supramolecular effects in comparing cellulose to GGM due to cellulose bundling into microfibrils whereas GGM does not. All generated models were solvated with explicit TIP3P (Jorgensen, 1983) water molecules. Where necessary in all simulations, charge neutrality was achieved by adding sodium cations and hydroxide or methanethiolate ions.

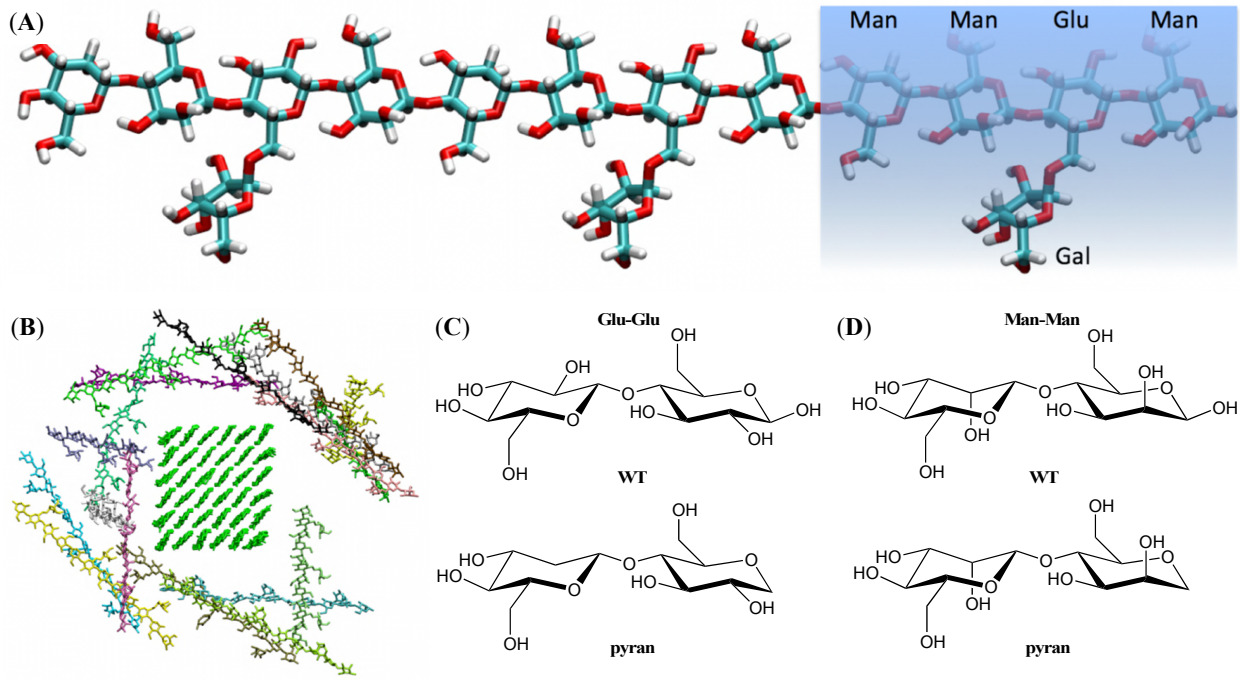

Figure 3. Atomistic models for MD simulation. (**A**) Model of galactoglucomannan (GGM) molecule composed of three repeating units (one repeating unit is shaded in blue), each consisting of three mannose, one glucose, and one galactose residue. (**B**) Edge-on view of an example starting configuration for a 36-chain cellulose microfibril (center, in green) randomly surrounded by 18 GGM molecules (various colors). (**C**) Wild-type Glu-Glu (glucose dimer) and Man-Man (mannose dimer). Note the difference in orientation of the hydroxy group at the O2 position between glucose and mannose. (**D**) Pretreated Glu-Glu and Man-Man dimers, in which the O1 hydroxy has been replaced by hydrogen to create an alkali-stable pyran species.

MD simulation details. All MD simulations were conducted using the program CHARMM (Brooks, 2009) with the CHARMM carbohydrate force field, *all36_carb* (Guvench, 2008; Hatcher, 2009). The DOMDEC fast parallel CHARMM method (Hynninen, 2014) was used to accelerate performance. All simulations used a 2 fs time step and the SHAKE algorithm (Kraeutler, 2001) to keep the length of covalent bonds to hydrogen fixed. Periodic solvated systems used a nonbonded cutoff of 11 Å, with a 2 Å list buffer and heuristic list update using a 1 Å switching function for dispersion, and the particle-mesh Ewald method (Darden, 1993) to calculate electrostatics accurately to long range. All systems were equilibrated with initial minimization and 200 ps constant pressure simulations (NPT) at 300 K. Subsequently, production runs of 300 ns for the GGM/cellulose microfibril complex and 100 ns for the dimeric systems were performed in the NVT ensemble.

Quantum mechanical model construction. Similar to the simplified models used in the classical MD simulations, we used a β-1,4 glucose dimer (Glu-Glu) to represent cellulose in the QM calculations. However, we used beta-(1,4)-linked Glu-Man as a model of GGM for the QM calculations of the alkaline hydrolysis reaction pathway because Man-Man is unable to undergo epoxide formation due to the stereochemistry at C2.

QM method validation. The dispersion-corrected hybrid meta-GGA density functional approximation M062X-D3 (Zhao, 2008) and the 6-31G (d,p) basis set were used throughout the study. M062X-D3 was chosen because it is among the top density functionals for calculating conformational energies of carbohydrates (Marianski, 2016), reaction energies for small systems, and noncovalent interactions in the

GMTKN55 benchmarks (Goerigk, 2017). As an additional evaluation of this model chemistry, we calculated the reaction free energy (ΔG_r) and water-assisted activation free energy (E_a) for the ring opening of cyclic alpha-D-glucose to form acyclic D-glucose. We obtained ΔG_r = 9.5 kcal/mol at the M062X-D3/6-31g(d,p) level of theory, which is in good agreement with the available reference value of 10.3 kcal/mol obtained at the CCSD(T)/G4 level of theory (Assary, 2012). Thus, we expect that the M062X-D3/6-31g(d,p) level of theory should provide sufficiently accurate energetics to investigate the model systems in the present work.

To account for solution-phase effects, we used the SMD polarizable continuum model (Marenich, 2009) with water as the solvent to calculate aqueous free energies. However, using the continuum solvent representation alone to calculate hydration free energies of charged solutes can be inaccurate. Thus, we included one or two explicit water molecules that interact directly with the solute to account for explicit hydrogen bonding. Vibrational frequencies were calculated for all optimized geometries to confirm the presence of zero or one imaginary frequencies for minima and transition states, respectively. Free energies were calculated within the rigid-rotor harmonic oscillator approximation at 298.15 K. All QM calculations were performed with Gaussian 16, revision A.03 (Frisch et al.).

Results and Discussion

Experimental kinetic data for real wood chips. We investigated the effectiveness of sodium methylmercaptide pretreatment in preserving carbohydrate yield from southern pine wood chips under a range of experimental conditions. Several parameters were adjusted to determine conditions that maximize carbohydrate yield and provide a kappa number in the target range of 25-30. A kappa number in this range is desirable because it is suitable for subsequent bleaching.

Table 1. Composition of pulp samples, rejects, and residual alkali.

	experimental conditions[a]		**composition (%)**[b]				**pulp yield (%)**				
	pretreatment	**pulp**	**xylan**	**GGM**	**cellulose**	**lignin**	**calc**[c]	**meas**[d]	**kappa number**	**% rejects**	**residual EA (g/L Na2O)**
0	southern pine chips		10.28	15.69	41.94	29.5	n/a	100			
1	0% MM 115°C (ctrl)	15% EA	4.42	3.63	34.98	1.86	n/a	n/a	29.4 ± 0.7	0.04 ± 0.02	7.7 ± 0.15
			composition (%) rel to ctrl				**rel pulp yield (%)**				
2	0% MM 115°C	16% EA	0.19	-0.03	-1.09	-0.35	-1.29	-1.1	25.1 ± 0.2	0.05 ± 0.00	9.3 ± 0.20
3	0% MM 115°C	17% EA	-0.04	-0.11	-0.71	-0.55	-1.42	-1.5	22.7 ± 0.5	0.06 ± 0.05	10.6 ± 0.20
4	3% MM 105°C	15% EA	0.41	0.28	-0.61	-0.39	-0.32	-0.4	19.1 ± 0.5	0.03 ± 0.02	9.5 ± 0.68
5	3% MM 105°C	12% EA	1.16	0.21	0.89	0.24	2.49	2.5	29.0 ± 0.8	0.01 ± 0.01	6.2 ± 0.04
6	3% MM 115°C	12% EA	0.88	0.12	1.84	0.06	2.9	2.9	30.0 ± 0.5	0.04 ± 0.00	5.6 ± 0.06
7	3% MM 130°C	12% EA	1.25	0.16	-0.11	0.38	1.67	2.1	29.7 ± 0.9	0.01 ± 0.01	5.8 ± 0.08
8	3% MM 130°C pH 10	12% EA	1.6	0.35	0.93	1.83	4.7	4.8	46.6 ± 1.3	0.23 ± 0.04	3.3 ± 0.23
9	3% MM 80°C 90 min	12% EA[e]	0.8	0.54	0.68	0.23	2.24	2.2	28.8 ± 2.1	0.05 ± 0.01	6.0 ± 0.10
10	6% MM 80°C 90 min	11% EA	1.13	0.13	0.03	0.16	1.44	1.4	26.3 ± 0.5	0.04 ± 0.03	6.4 ± 0.15
11	1% MM 115°C	14% EA	0.64	0.02	-0.05	0.03	0.63	0.6	26.5 ± 0.4	0.00 ± 0.00	7.0 ± 0.13
12	6% MM 115°C	9% EA	1.78	0.46	2.17	1.34	5.74	5.8	40.1 ± 0.8	0.33 ± 0.05	4.3 ± 0.01
13	6% MM 115°C	11% EA	1.17	0.12	1.84	-0.21	2.92	2.9	25.9 ± 0.3	0.02 ± 0.00	6.5 ± 0.15
14	3% MM 115°C	12% EA	0.69	0.26	1.58	0.1	2.63	2.6	27.5 ± 0.4	0.03 ± 0.02	6.2 ± 0.22
15	6% MM 115°C	10% EA	1.27	-0.04	1.24	0.22	2.68	2.7	29.6 ± 1.4	0.12 ± 0.17	5.6 ± 0.22

[a] All reactions were carried out at 1 mM NaOH, pH 12, for 60 minutes unless otherwise stated.
[b] based on dry wood mass
[c] Calculated from pulp analysis data
[d] Measured from pulp yield data
[e] No impregnation

We first measured xylan, GGM, cellulose and lignin compositions for southern pine chips prior to pulping and obtained yields of 10.3% xylan, 15.7% GGM and 41.9% cellulose (**Table 1**). Under pulping conditions of 1 mM NaOH, 115℃, pH 12 for 60 minutes, we obtained a kappa number of 29.4 +/- 0.7 when the effective alkalinity (EA) was 15% (**Table 1**, condition 1). Under these conditions, the compositions of xylan, GGM, and cellulose were reduced to 4.4, 3.6, and 35.0, respectively.

We then analyzed the effect of changing the EA on kappa number to identify pulping conditions that led to kappa numbers in the desired range (**Table 1** and **Figure 4**). As expected, there is a linear relationship between total pulp yield and kappa number for the control cooks (**Figure 4**). Increasing EA to 16% (cond 2) and 17% (cond 3) resulted in reduction of the kappa number to 25.1 +/- 0.2 and 22.7 +/- 0.5, respectively. Thus, we selected condition 1 as the control.

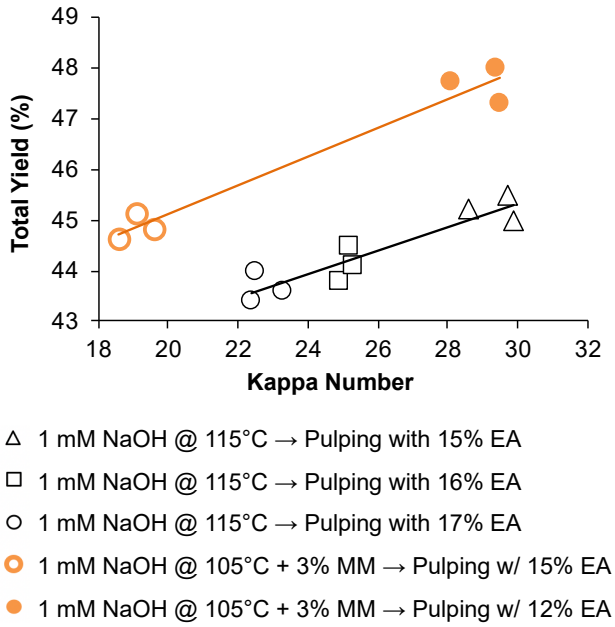

Figure 4. Kappa number versus yield for unpretreated samples (conditions 1-3 in **Table 1**) and for samples pretreated with 3% MM at 105°C (conditions 4-5).

Next, we considered the effects of MM pretreatment and also varied the temperature, pH, reaction time, and effective alkalinity. For most of the experiments there is good agreement between the calculated and experimentally measured pulp yield increase (**Table 1**). The amount of rejects were less than 0.1% except for two experiments, pre-treatment with 3% MM (pH 10) liquor followed by pulping with 12% EA (0.23% rejects, condition 8) and pre-treatment with 6% MM liquor followed by pulping with 9% EA (0.33% rejects, condition 12). The residual alkali was generally within the acceptable ranges of 4-10 g/L.

The initial MM pretreatment experiments were performed at a charge of 3% MM on o.d. wood for 60 minutes at 105°C (condition 4). The temperature of 105°C was chosen assuming that, at this temperature and pH ~12 of the pretreatment liquor, the kinetics of the primary peeling reactions of GGM and cellulose would be slow enough compared to the kinetics of the reducing end group stabilization reactions of MM. Under these pretreatment conditions with 15% EA, the kappa number dropped to 19.1.

Therefore, to obtain a kappa number that is closer to the target value, we performed a 12% EA cook after pretreatment with 3% MM (condition 5) and obtained a kappa number of 29. The results show that the

addition of MM increased the retention of wood carbohydrates with an increase of ~2.5% in the pulp yield with the same kappa as the control. It is also important to note that the 3% MM pretreatment allowed decreasing the EA charge in kraft cooking from 15% to 12% while still achieving the same kappa number as the control kraft cook at 15% EA. Under these conditions we observed substantial increases in the yields of xylan (1.16%) and cellulose (0.89%), but only a negligible increase in the GGM yield (0.21%). In addition, there is good agreement between pulp yields calculated from the pulp composition and the measured values. This agreement indicates a good mass balance closure and accurate and reproducible chemical and experimental methods, respectively.

Next, we increased the temperature in condition 5 to 115°C (condition 6). We observed a 1.8% increase in cellulose yield relative to the control, but only a 0.1% increase in GGM yield. Increasing the temperature to 130°C (condition 7) results in a slight reduction in the cellulose yield, probably due to peeling reactions. Reducing the pH from 12 in condition 7 to 10 (condition 8) results in increases of xylan, GGM and cellulose, but with a substantial increase in kappa to 46.6.

We hypothesized that the MM stabilization reaction of cellulose occurs during the 60-minute impregnation phase at 115°C, but unfortunately the stabilization reaction of GGM by MM is too slow compared to the GGM primary peeling reaction to affect the retention of GGM. Increasing the cooking time from 60 to 90 minutes, reducing the temperature to 80°C, and skipping the impregnation step (condition 9) leads to small increases in the yields of xylan (0.8%), GGM (0.5%) and cellulose (0.7%) relative to the control while also maintaining a kappa number of 28.8. Decreasing the temperature in conditions 5 (105°C) and 6 (115°C) to at 80°C (conditions 9 and 10) resulted in the retention of less cellulose, which might suggest that the stabilization of cellulose by MM at 80°C is too slow to retain additional cellulose. We also increased the MM to 6%, along with EA = 11% (condition 13). Under these conditions, we observed a substantial increase in cellulose yield relative to the control (1.8%), but essentialy no change in GGM yield.

The amount of xylan retention was mostly related to alkali charge because more xylan is dissolved at higher alkaline concentrations. The experiments with 3% MM pretreatment at 130°C (conditions 7 and 10) resulted in a higher retention of xylan, presumably because more alkali was consumed by cellulose peeling, which in turn lowered the solubility of xylan in the cooking liquor. The amount of GGM retained was very small even for the experiments with pretreatment at 80°C (conditions 8 and 9). Since primary peeling of GGM starts at about 80°C (Montagna, 2013), while primary peeling of cellulose is only significant at 130°C (Paananen, 2010; Nieminen, 2014) it is possible that MM stabilizes some cellulose before peeling but that GGM stabilization by MM is too slow compared to primary peeling. Based on absolute pulp yield increase (**Table 1**), the optimal conditions for MM use is to add it directly to white liquor at a charge of 3% (w/w) on wood (as MM).

Molecular dynamics (MD) simulations. Molecular dynamics (MD) simulations were performed to determine the spatial distributions of ionic additives of the pretreatment chemistry around each biomass polysaccharide. In addition, MD simulations are used to determine the analogous distributions of the ions that are formed upon dissociation of the active alkaline species that perform peeling reactions (NaOH and Na_2S in aqueous solution). The interactions of these ions were probed with the unmodified forms of cellulose and hemicellulose as well as with the corresponding forms modified by pretreatment.

Cellulose/GGM simulations. A 300 ns simulation of a GGM/cellulose microfibril complex under peeling conditions, i.e., in the presence of NaOH (**Figure 5**) was performed to investigate the distribution of OH^- ions, which are responsible for peeling reactions. Simulations at both 0.9 M and 1.5 M NaOH indicate that OH^- ions have a much higher propensity to bind to the reducing end of GGM than to cellulose, as revealed by comparing the two radial distribution functions (**Figure 5C**). We note that thermodynamic quantities were not directly computed. This difference in affinity could be due to the chemical differences between

cellulose and GGM or to the crystalline nature of cellulose possibly rendering physical protection against peeling.

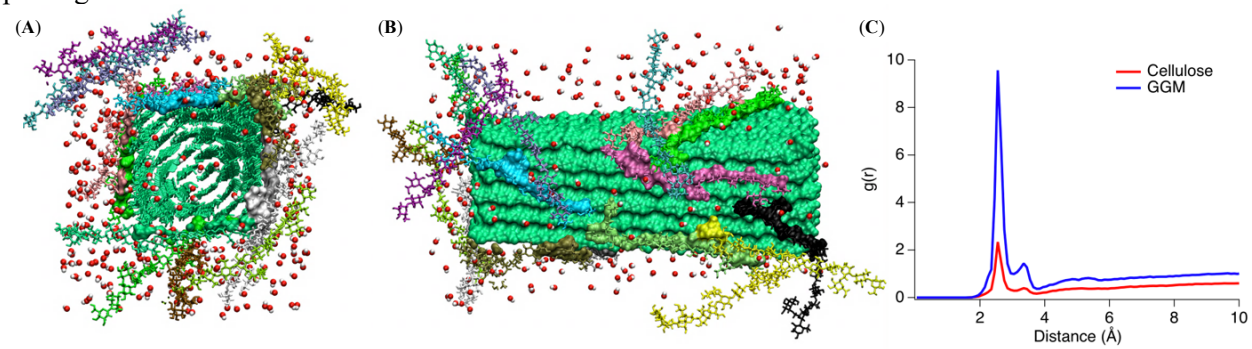

Figure 5. Snapshot of the GGM/cellulose complex at the end of a 300 ns MD simulation. (**A**) End-on view and (**B**) side view rotated 90 degrees with cellulose microfibril shown in green surface representation and bound GGM residues shown in solid surface model of various colors. Unbound GGM residues are shown in stick representation. Hydroxide ions are shown as spheres (red: oxygen, white: hydrogen). (**C**) Radial distribution function of OH^- ions with respect to O1 and O2 at the reducing end of cellulose or GGM. Results shown are with NaOH concentration of 0.9 M; 1.5 M NaOH loading showed qualitatively similar behavior.

Dimer simulations under peeling conditions. The higher affinity of hydroxide ions for GGM than for cellulose (as deduced from radial distribution functions) was also observed in 100 ns simulations of Glu-Glu and Man-Man dimers (**Figure S1**). Glucose and mannose differ only in the stereochemistry at the C2 carbon, and our results demonstrate that OH^- ions exhibit a stronger propensity to localize at the bridging position between the O1-O2 atoms in mannose (**Figure S1**), possibly promoting more substantial peeling of mannose (and thus in GGM) than glucose, even in the absence of supramolecular structure (i.e., cellulose microfibril). Analogous simulations with pretreated dimers indicate that OH^- ions retain a stronger affinity to the hydroxy group in mannose, but in this case around the O2-O3 atoms (**Figure S1**). This enhanced affinity is possibly due to *cis*-OH groups at these two carbon ring atoms and may promote both the peeling reaction in the WT Man-Man dimer and the dehydration reaction in the pretreated Man-Man dimer.

Dimer simulations under pretreatment conditions. Next, we examined the distribution of CH_3S^- ions, which form upon dissociation of sodium methyl mercaptan. These ions perform the pretreatment reactions, and, similar to the hydroxide ions described above, they exhibit affinity for the C1 atom in both Glu-Glu and Man-Man dimers. This position may be favorable for the nucleophilic S_N2 reaction that accomplishes the conversion to alkali stable end group and tends to be slightly higher in glucose than mannose (**Figure 6**).

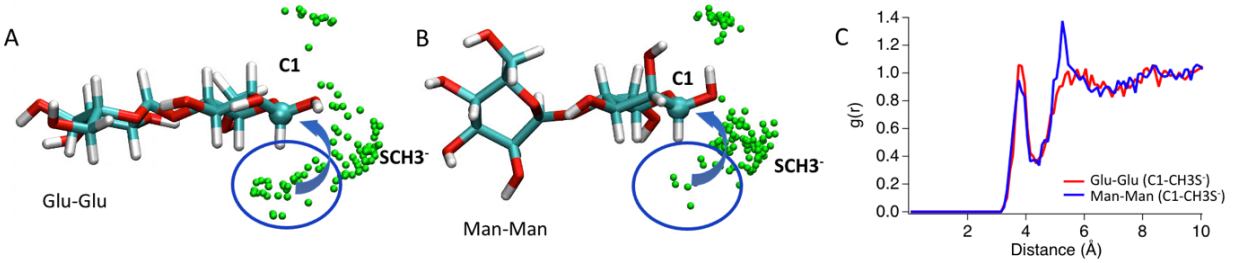

Figure 6. Simulations of pretreated Glu-Glu and Man-Man dimers in MM solution. Snapshots of CH_3S^- ions around C1 at the reducing end of (**A**) a Glu-Glu dimer and (**B**) Man-Man dimer. (**C**) Radial distribution function of CH_3S^- ions with respect to C1 at the reducing end of a Glu-Glu (red) or Man-Man (blue) dimer (CH_3S^- concentration = 1.5 M).

Lastly, MD simulations of the cellulose microfibril with GGM molecules described above also may shed some insight into the higher susceptibility of GGM to secondary hydrolysis. **Figure 7** shows the radial distribution for OH^- ions with respect to the glycosidic oxygen (O4) of cellulose and GGM, the site of initiation for alkaline hydrolysis. The results indicate a much higher local concentration of OH^- ions around O4 in GGM than cellulose. This effect is likely due to protection provided by the microfibrillar structure of cellulose that is not afforded to GGM.

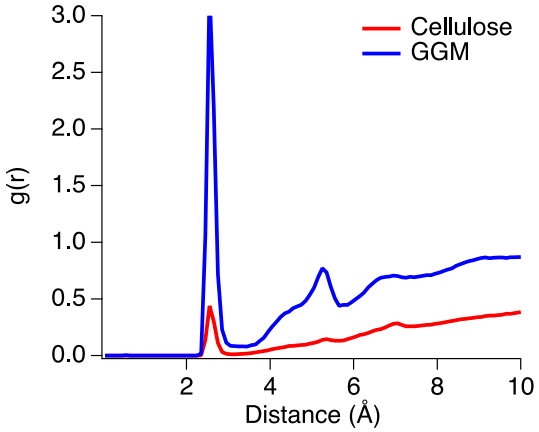

Figure 7. Radial distribution function of OH^- ions at the glycosidic bond (O4 atom) in cellulose and GGM dimer models.

Reactive MD under peeling and pretreatment conditions. In addition to purely classical MD simulations, reactive MD simulations at various operating conditions allowed for characterization of reactive configurations for peeling and pretreatment. High-fidelity reactive force fields for the species and operating conditions of interest are not available, but the purpose of these simulations is not a faithful reproduction of reaction energetics. Rather, reactant and intermediate configurations obtained from reactive MD were subsequently examined with density functional theory (DFT)-based mechanistic studies as described below. ReaxFF (van Duin, 2001), a reactive force field wherein the breaking and forming of chemical bonds is captured, has been developed and applied for a wide range of systems to examine the chemical evolution of these systems at the atomistic level. (Senftle, 2016; Han, 2016)

ReaxFF simulations were conducted to initiate the study of the reaction mechanism for the β-hydroxycarbonyl elimination reaction, i.e., the breaking of the β-1,4 bond, using intermediate P3 of a Glu-Glu dimer as the model compound (**Figure 3**). After testing three different ReaxFF force field variants (Rahnamoun, 2014; Monti, 2013a; Monti, 2013b), we selected the variant that demonstrated the tendency to break β-1,4 bonds preferentially over C-C bonds. The system contains one Glu-Glu dimer and 21 NaOH, corresponding to a concentration of 2 M NaOH. All reactive simulations were conducted in the NVT ensemble at 300 K for 10 ps with a time step of 0.1 fs. Of the 100 independent ReaxFF MD simulations conducted, glycosidic bond cleavage occurred in 75. Snapshots of one illustrative example of a reactive MD trajectory (not shown) indicate that it proceeded through the following steps for β-1,4 bond breaking: (**B**, **C**) proton transfer between O3 and O5; (**D**) C1-O5 bond breaking; (**E**) β-1,4 bond cleavage; and (**F**) dehydration at C5.

Quantum mechanical calculations of peeling and pretreatment reactions

QM calculations were carried out to determine the energy profiles of both wood polysaccharides, cellulose and GGM, under kraft pulping conditions, including primary peeling, stopping, pretreatment, and secondary peeling reactions. These calculations can provide additional fundamental understanding of kraft pulping,

the reasons for the undesired loss of GGM even after MM pretreatment and may provide insights into the design of pretreatment agents that can better preserve GGM during kraft pulping.

Primary peeling. Alkali-catalyzed endwise degradation, or primary peeling, is a major cause of the loss of carbohydrates during kraft pulping. The generally accepted mechanism of primary peeling is shown in **Figure 9**. The main steps include: (i) ring opening to form an aldehyde, (ii) aldose-ketose transformation (i.e., enolization), (iii) β-elimination, (iv) tautomerization, and (v) benzylic acid rearrangement (Sixta, 2006). Our aim is to limit (or ideally, prevent) primary peeling, necessitating a detailed mechanistic understanding of this process. Thus, we calculated a reaction pathway for the primary peeling reactions according to this accepted reaction mechanism. We generated reaction free energy diagrams for these five steps with both Glu-Glu and Man-Man (**Figure 10**).

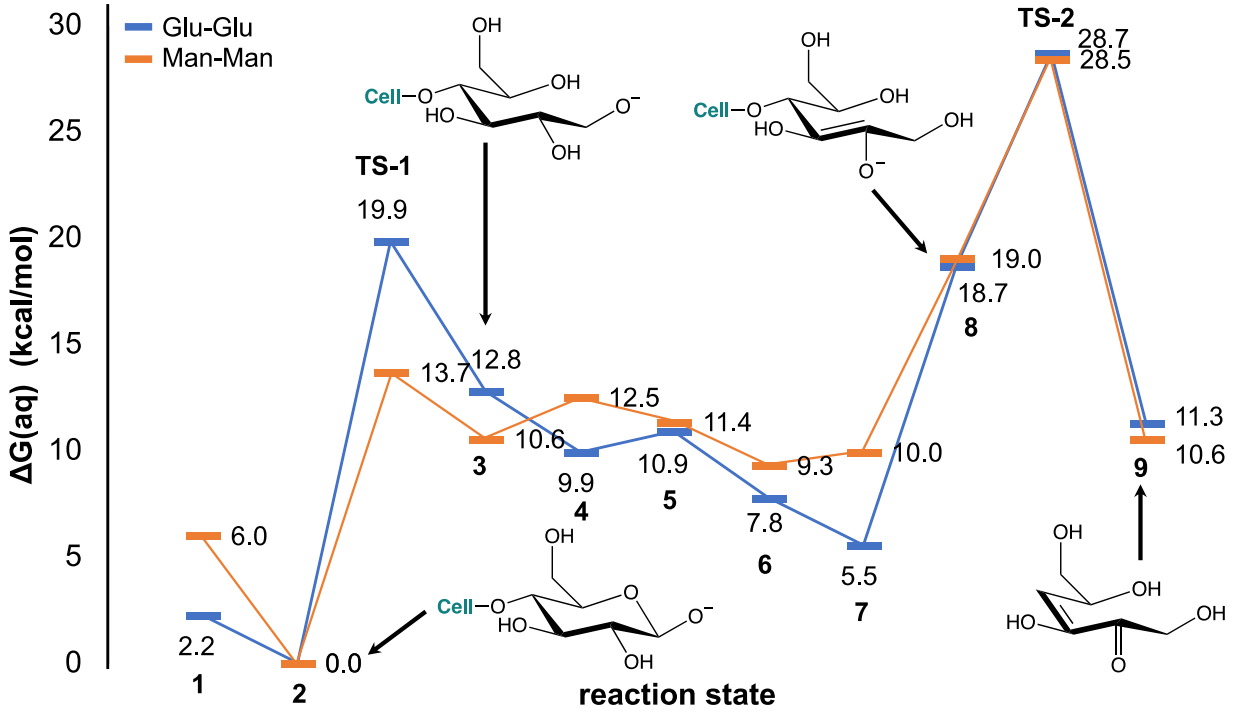

Figure 9. Free energy profiles for primary peeling mechanism for (**A**) Glu-Glu (representing cellulose) and (**B**) Man-Man (representing GGM). Structures for select states for GG are shown.

The calculated activation energies (E_a) for primary peeling of the Glu-Glu and Man-Man models are 28.7 and 28.5 kcal/mol, respectively, which we consider to be essentially equivalent. These barriers were calculated as the difference in free energy between the low-energy reactant state ("cyclic⁻" in **Figure 10**) and that of the transition state for peeling ("P-TS-1" in **Figure 10**).

Alkaline hydrolysis. To investigate the mechanism and energetics of alkaline hydrolysis in dimeric cellulose and GGM models, we calculated a reaction pathway for the generally accepted mechanism of alkaline hydrolysis of Glu-Glu (cellulose model) and Glu-Man (GGM model), with a particular emphasis on the energetics of converting the O2-deprotonated species to the epoxide intermediate (**Figure 9**). We found that the free energy barrier for the formation of the epoxide is 41.8 kcal/mol for Glu-Glu and 39.1 kcal/mol for Glu-Man (**Table 2**). Thus, the calculated barrier for Glu-Man is ~2 kcal/mol lower than for Glu-Glu, suggesting that GGM could potentially be slightly more readily hydrolyzed. However, it is important to note that such a small energy difference is within the error of the method. Furthermore, the models are dimeric representations of much larger polymers so we are reluctant to make firm conclusions about the relative susceptibility to alkaline hydrolysis in these two systems.

Table 2. Calculated free energies for alkaline hydrolysis of GG and MM relative to cyclic-anion-bb.

	relative free energy (kcal/mol)	
model	**Glu-Glu**	**Glu-Man**
cyclic-anion-bb	0.0	0.0
cyclic-anion-cb	0.6	3.9
eyclic-epoxide-ts	41.8	39.1
cyclic-epoxide	17.8	20.1

Discussion

Softwood pretreatment with methyl mercaptide (MM) has been demonstrated to increase yield by 3%, primarily by stabilizing carbohydrates against degradation by peeling (**Table 1**). Unfortunately, GGM stabilization by this pretreatment is minimal, and thus represents a promising target for increasing the overall preservation of wood carbohydrates and improved yields. GGM has an initial degree of polymerization (DP) of ~200 and the loss by primary peeling during impregnation with NaOH and Na_2S is ~50-60%. Further glucomannan loss occurs due to secondary peeling, or peeling that occurs after alkaline hydrolysis of a polysaccharide chain creates a new chain end. As a result, the final kraft pulp contains only ~25% of the native glucomannan. The dissolution of xylan is governed mostly by alkaline solubility of the residual polymers because the uronic acid side group protects xylan from extensive peeling. Therefore, the estimated pulp yield increase from avoiding primary peeling is ~12% for softwoods (4% cellulose, 8% GGM) and ~6% for hardwoods (4% cellulose, 2% glucomannan).

Wood remains the largest cost in the manufacture of wood pulp for paper, making up over half of the non-capital operating cost of producing pulp. Therefore, increasing pulp yield would have a major financial impact on pulp mill economics. Unfortunately, despite intensive R&D efforts, attempts to increase kraft pulp yield have not yet reached the desired level. In general, pulp yield is less than 50% compared to a potential maximum yield of 70-75% when both cellulose and hemicelluloses are fully retained.

The application of a variety of molecular modeling techniques yielded several key findings. Classical MD simulations of biomass polysaccharides cellulose and GGM indicate that OH^- ions have a greater propensity to localize near the reducing end of GGM than cellulose, suggesting that the crystalline nature of cellulose may provide physical protection against peeling. In addition, MD simulations of glucose and mannose dimers (representing cellulose and GGM, respectively) revealed an enhanced prevalence of OH^- ions in regions that could promote peeling in GGM, even when the end group is converted to an alkali-stable thioether functionality. QM calculations indicate that the peeling reactions for cellulose and GGM models have similar energetic profiles for the glucose and mannose models. Thus, we suspect that the reason GGM is less well preserved by pretreatment is that it has more hydrolytically accessible sites due to its less crystalline structure. This internal chain scission is important because it leads to the creation of new reducing end groups that can subsequently undergo depolymerization, a phenomenon known as secondary peeling. Thus, even though reducing end groups may be protected initially through pretreatment, new (unprotected) reducing end groups may be generated during pulping. If secondary hydrolysis is indeed the primary mechanism for GGM yield loss, it is possible that co-treatment with MM during kraft pulping could be carried out to cap newly created REGs as they are formed through alkaline hydrolysis. These findings provide valuable insight that can inform future studies aimed at improving carbohydrate yield through novel pretreatment strategies.

These findings and others will be described in a forthcoming peer-reviewed journal publication.

Subject Inventions (As defined in the CRADA)

None.

Commercialization Possibilities

None.

Plans for Future Collaboration

None.

Conclusions

The Contractors performed extensive computational chemistry calculations and complementary lab experiments to establish a thorough understanding of pretreatment methods. This insight was intended to provide new insight that will ultimately lead to improved pulping efficiency.

References

Nieminen, K.; Paananen, M.; Sixta, H., *Ind Engin Chem Res,* **2014,** *53*, 11292-11302.

Paananen, M.; Tamminen, T.; Nieminen, K.; Sixta, H., *Holzforschung* **2010,** *64*, 683-692.

Montagna, P. N.; Inalbon, M. C.; Paananen, M.; Sixta, H.; Zanuttini, M. A., *Ind Engin Chem Res,* **2013,** *52*, 3658-3662.

Fearon, O.; Nykänen, V.; Kuitunen, S.; Ruuttunen, K.; Alén, R.; Alopaeus, V.; Vuorinen, T.; *AIChE J.*, **2020**, 66, e16252.

Silva-Perez et al., *Cellulose*, **2015**, 22:3967–3979.

Kraütler et al., *Carb Res,* **2007**, 342, 2097–2124.

Peric-Hassler et al., *Carb Res*, 2010, 345, 1781–1801.

Berglund, 2016, *Plant J*, **2016**, 88, 56–70.

Scott, R. W., *Analytical chemistry* **1979,** *51*, 936-941.

Negahdar, L.; Delidovich, I.; Palkovits, R., *Appl Catal B: Environ,* **2016,** *184*, 285-298.

Jorgensen, W. L.; Chandrasekhar, J.; Madura, J. D.; Impey, R. W.; Klein, M. L., *J Chem Phys,* **1983,** *79*, 926-935.

Brooks, B.R. et al. *J. Comput Chem*, **2009**, 30, 1545-1614.

Guvench, O.; Greene, S. N.; Kamath, G.; Brady, J. W.; Venable, R. M.; Pastor, R. W.; Mackerell, A. D., *J Comput Chem,* **2008,** *29*, 2543-2564.

Hatcher, E. R.; Guvench, O.; MacKerell Jr, A. D., *J Chem Theory Comput,* **2009,** *5*, 1315-1327.

Hynninen, A. P.; Crowley, M. F., *J Comput Chem,* **2014,** *35*, 406-413.

Kräutler, V.; Van Gunsteren, W. F.; Hünenberger, P. H., *J Comput Chem* **2001,** *22*, 501-508.

Darden, T.; York, D.; Pedersen, L., *J Chem Phys,* **1993,** *98*, 10089-10092.

Zhao, Y.; Truhlar, D. G., *Theor Chem Acc,* **2008,** *120*, 215-241.

Marianski, M.; Supady, A.; Ingram, T.; Schneider, M.; Baldauf, C., *J Chem Theory Comput,* **2016,** *12*, 6157-6168.

Goerigk, L.; Hansen, A.; Bauer, C.; Ehrlich, S.; Najibi, A.; Grimme, S., *Phys Chem Chem Phys,* **2017,** *19*, 32184-32215.

Assary, R. S.; Curtiss, L. A., *Energy Fuels* **2012,** *26*, 1344-1352.

Marenich, A.; Cramer, C. J.; Truhlar, D. G. *J. Phys. Chem. B,* **2009**, 113, 18, 6378–6396.

Frisch, M. J. et al.. Gaussian 16 Rev. C.01, Wallingford, CT, 2016.

Van Duin, A. C.; Dasgupta, S.; Lorant, F.; Goddard, W. A., *J Phys Chem A,* **2001,** *105*, 9396-9409.

Senftle, T. P.; Hong, S.; Islam, M. M.; Kylasa, S. B.; Zheng, Y.; Shin, Y. K.; Junkermeier, C.; Engel-Herbert, R.; Janik, M. J.; Aktulga, H. M., *Comput Mater* **2016,** *2*, 15011.

Han, Y.; Jiang, D.; Zhang, J.; Li, W.; Gan, Z.; Gu, J., *Front Chem Sci Engin,* **2016,** *10*, 16-38.

Rahnamoun, A.; Van Duin, A., *J Phys Chem A,* **2014**, 118, 2780-2787.

Monti, S.; Corozzi, A.; Fristrup, P.; Joshi, K. L.; Shin, Y. K.; Oelschlaeger, P.; van Duin, A. C.; Barone, V., *Phys Chem Chem Phys*, **2013**, 15, 15062-15077.

Monti, S.; Li, C.; Carravetta, V., *J Phys Chem C*, **2013**, 117, 5221-5228.